



Er/O and Er/F doping during molecular beam epitaxial growth of Si layers for efficient 1.54 μm light emission

W.-X. Ni, K. B. Joelsson, C.-X. Du, I. A. Buyanova, G. Pozina, W. M. Chen,, G. V. Hansson, B. Monemar, J. Cardenas, and B. G. Svensson

Citation: *Applied Physics Letters* **70**, 3383 (1997); doi: 10.1063/1.119178

View online: <http://dx.doi.org/10.1063/1.119178>

View Table of Contents: <http://scitation.aip.org/content/aip/journal/apl/70/25?ver=pdfcov>

Published by the AIP Publishing

Articles you may be interested in

[Growth-temperature dependence of Er-doped GaN luminescent thin films](#)

Appl. Phys. Lett. **80**, 344 (2002); 10.1063/1.1434312

[Effect of O:Er concentration ratio on the structural, electrical, and optical properties of Si:Er:O layers grown by molecular beam epitaxy](#)

J. Appl. Phys. **88**, 4091 (2000); 10.1063/1.1308093

[Er doping of GaN during growth by metalorganic molecular beam epitaxy](#)

Appl. Phys. Lett. **72**, 2710 (1998); 10.1063/1.121107

[Properties of Er-related emission in in situ doped Si epilayers grown by molecular beam epitaxy](#)

J. Vac. Sci. Technol. B **16**, 1732 (1998); 10.1116/1.590044

[Room temperature 1.54 \$\mu\text{m}\$ light emission of erbium doped Si Schottky diodes prepared by molecular beam epitaxy](#)

Appl. Phys. Lett. **71**, 1023 (1997); 10.1063/1.119715

The banner features the AIP Applied Physics Reviews logo on the left, which includes a small image of a crystal structure. To the right, the text 'NEW Special Topic Sections' is prominently displayed in white against a blue background with a glowing light effect. Below this, the text 'NOW ONLINE' is in yellow, followed by 'Lithium Niobate Properties and Applications: Reviews of Emerging Trends' in white. The AIP Applied Physics Reviews logo is also present in the bottom right corner.

NEW Special Topic Sections

NOW ONLINE
Lithium Niobate Properties and Applications:
Reviews of Emerging Trends

AIP Applied Physics Reviews

Er/O and Er/F doping during molecular beam epitaxial growth of Si layers for efficient 1.54 μm light emission

W.-X. Ni,^{a)} K. B. Joelsson, C.-X. Du,^{b)} I. A. Buyanova, G. Pozina, W. M. Chen,
G. V. Hansson, and B. Monemar

Department of Physics, Linköping University, S-581 83 Linköping, Sweden

J. Cardenas and B. G. Svensson

Department of Electronics, Royal Institute of Technology, Electrum 229, S-164 40 Kista-Stockholm, Sweden

(Received 27 January 1997; accepted for publication 16 April 1997)

Er, together with oxygen or fluorine as co-dopants, has been incorporated into Si during molecular beam epitaxial growth using co-evaporation of Si and Er containing compounds. The Er doping concentration using both Er_2O_3 and ErF_3 can reach a level of $\sim 5 \times 10^{19} \text{ cm}^{-3}$ without precipitation, which is at least one order of magnitude higher than a previously reported solid solubility limit for Er in Si. Growth, structural, and luminescence characterization of these Er/O and Er/F doped Si samples are reported. In particular, 1.54 μm electroluminescence has been observed from Er/O doped Si layers at room temperature through hot electron impact excitation. © 1997 American Institute of Physics. [S0003-6951(97)00425-7]

Monolithically integrating optoelectronic devices and conventional integrated circuits (ICs) onto one Si chip using mature Si technology is a long sought after goal for microelectronics industry to produce novel ICs, e.g., optical interconnects, with high reliability and low cost. An efficient light emitting device fabricated using Si-based materials is, however, so far still missing. Due to an internal transition between 4f states of Er ions, Er dopants in Si are known to give luminescence at 1.54 μm ,¹ which is a wavelength commonly used in optical fiber communication. Recent observations of room temperature electroluminescence (EL) from Er doped Si structures by several research groups²⁻⁴ indicate that Er-doped Si can be a promising material for Si-based optoelectronics.

Some problems still remain which limit the use of Er doping in Si. The reported maximum concentration of Er atoms in the Si matrix without precipitation was about $1 \times 10^{18} \text{ cm}^{-3}$ when Xie *et al.*⁵ concluded that this concentration limit made Er doping not useful for device applications. At the same time, for efficient light emission from Er ions, some co-dopants, e.g., oxygen or fluorine, may be necessary⁶ in order to enhance Er excitation through a so-called carrier-mediated process and also to reduce the concentration of the deeper energy levels, induced by Er doping, close to the middle of the Si band gap. A conventional way to incorporate Er together with such co-dopants is using ion implantation. In this case, a high temperature annealing is necessary to activate Er atoms and also to remove the implantation-induced lattice damage. Furthermore, Er trapping at defect sites, which limits the maximum active Er incorporation and Er segregation towards the surface during annealing, have been reported.⁷ Improvement of the Er incorporation in high quality crystalline Si is thus a very crucial material issue for research.

Some low temperature techniques including growth of

Er doped Si layers by molecular beam epitaxy (MBE) under an oxygen ambient,^{4,8} and ion beam epitaxy⁹ have shown possibilities of increasing Er incorporation to a range of 10^{19} cm^{-3} and decrease Er surface segregation. In particular MBE grown Er-doped Si layers have been of interest due to recently promising luminescence results.⁴ In this letter, we report a study of direct incorporation of Er together with oxygen or fluorine during MBE growth by using co-evaporation of Si and erbium compound materials, namely Er_2O_3 and ErF_3 . The grown Er-doped Si layers were characterized *in situ* by reflection high-energy electron diffraction (RHEED), low-energy electron diffraction (LEED), and Auger electron spectroscopy (AES), and after growth by secondary ion mass spectrometry (SIMS), photoluminescence (PL), EL, and cross-sectional transmission electron microscopy (XTEM) measurements.

All growth experiments were carried out in a Vacuum Generators V-80 Si-MBE system at substrate temperatures between 350 and 600 °C with Si deposition rates of 0.5–1 Å s⁻¹. The Er flux together with oxygen or fluorine atoms was supplied by sublimation of Er_2O_3 or ErF_3 using high temperature effusion cells developed and fabricated by our group.¹⁰ The temperature used for sublimation ranges from 1500 to 1900 °C for Er_2O_3 , and between 1000 and 1400 °C for ErF_3 .

It has been noted that there is a significant, temperature dependent, surface roughening associated with surface segregation of Er and co-dopants during the growth of Er doped layers, which in turn degrades the growth quality of the layers. This was evidenced by *in situ* RHEED, LEED, and AES observations. For Er_2O_3 doped samples, the growth at 420 °C can in general be maintained in a two dimensional (2D) mode (a 2×1 reconstruction was observed by RHEED) with a moderate Er_2O_3 flux corresponding to an equivalent bulk Er concentration of $1 \times 10^{19} \text{ cm}^{-3}$. Above this concentration, the RHEED pattern degraded, implying a more severe surface roughness. The RHEED pattern eventually developed to be bulklike when the Er bulk doping concentration exceeded $2 \times 10^{20} \text{ cm}^{-3}$. The LEED observations showed that the rough surface contained some {311} facets. Increasing the

^{a)}Corresponding author; Tel: +46-13 282474; Fax: +46 13 137568; Electronic mail: wxn@ifm.liu.se

^{b)}Permanent address; Dept. of Electronic Engineering, Beijing Polytechnic University, Beijing 100022, People's Republic of China.

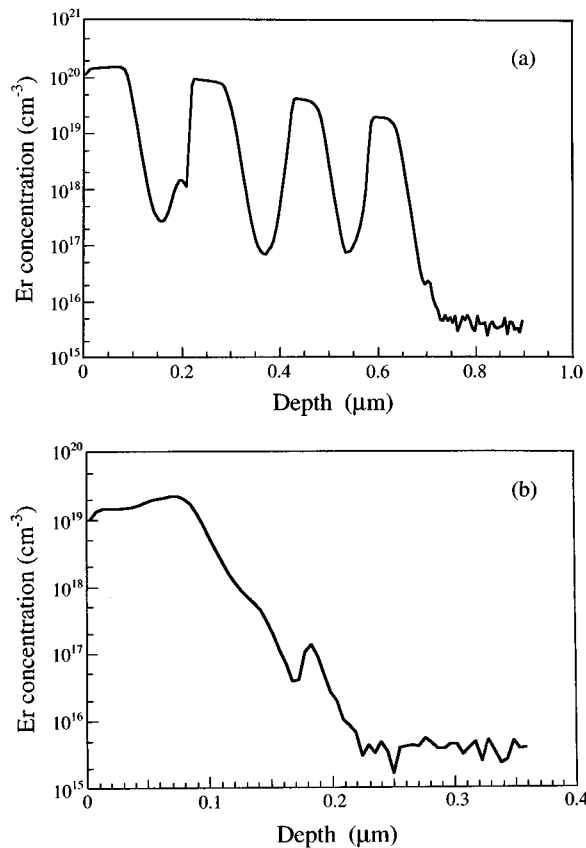


FIG. 1. SIMS profiles of the Er concentration (a) in a modulation doped sample grown at 420 °C where the first two layers were free of defects as judged from XTEM studies, and (b) in a single doping layer grown at 500 °C where surface segregation induced Er profile broadening is clearly observed. The sharp low intensity peaks in the profiles are due to growth interruptions.

growth temperature may improve the surface roughness, but the Er doping profile will be smeared out due to Er segregation.

Figure 1(a) shows an Er SIMS profile obtained from a multilayer sample grown at 420 °C with different Er_2O_3 impinging fluxes. Well defined Er doping layers with the highest Er doping concentration of $1.5 \times 10^{20} \text{ cm}^{-3}$ indicate a low segregation effect. The oxygen concentration of this sample was also profiled (not shown) using a Cs^+ beam. The O concentrations corresponding to the Er doped layers (from the surface) were 2.4×10^{20} , 1.2×10^{20} , 9×10^{19} , and $6.5 \times 10^{19} \text{ cm}^{-3}$, respectively. A ratio of O/Er that is larger than 1.5 for lower Er doping concentrations is due to a high oxygen background ($\sim 5 \times 10^{19} \text{ cm}^{-3}$) during SIMS measurements. From XTEM of this sample, it was evident that the two first layers appear to be free of any defects, while the two layers with highest Er concentrations contain an increasing number of precipitates.¹¹ The top surface of the sample was also rough, which is consistent with the *in situ* RHEED and LEED observations. It can thus be concluded that the incorporation limit has been increased by at least one order of magnitude relative to the previously reported value. Such an improvement is important for device applications, e.g., lasers. At the same time, it has been noted that for a sample grown at 500 °C, there is a significantly broadened deep tail of the doping profile due to Er segregation [Fig. 1(b)].

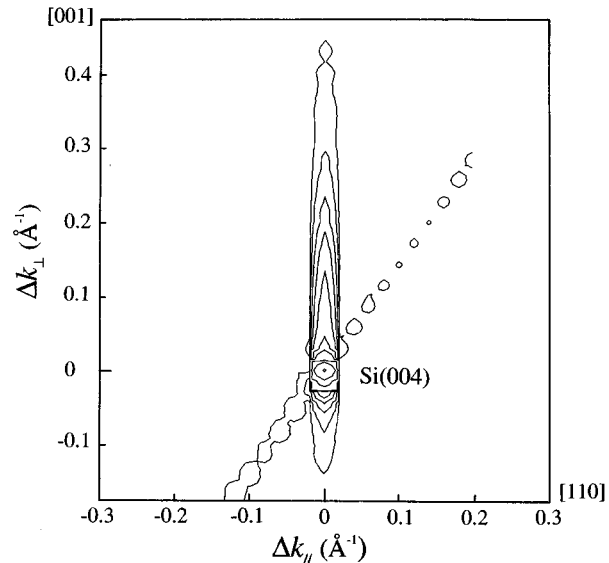


FIG. 2. A 2D reciprocal space map of HRXRD at around the (004) reflection from an Er doped layer characterized in Fig. 1(b). Tensile rather than compressive strain is observed from this sample with moderate Er/O doping concentration.

The strain in these Er/O doped samples has been characterized by reciprocal space mapping of HRXRD¹² and a resulting (004) map is shown in Fig. 2 ($N_{\text{Er}} \approx 2 \times 10^{19} \text{ cm}^{-3}$). Despite the large size of the Er atoms or any ErO_x complex, there is a tensile strain in the Er doped layer as evidenced by the observation of an asymmetrical broadening of the diffraction peak towards the direction of increasing k_{\perp} . The lack of mosaic broadening, i.e., broadening in the k_{\parallel} direction, indicates that the doped layer was grown pseudomorphically without generation of misfit dislocations or other extended defects.

The situation for ErF_3 doping in Si is somewhat different. First, the effect of accumulating surface roughening during the growth was much stronger at 400 °C. Therefore, it was more difficult to grow a thick Er/F doped layer without severe defect incorporation and Er precipitation via defect trapping. To overcome this problem, structures have been prepared by alternating growth at a lower temperature (350 °C) with ErF_3 flux and at a higher temperature (600 °C) without ErF_3 flux. In this way, 2000-Å-thick layers with average concentrations of $N_{\text{Er}} > 10^{19} \text{ cm}^{-3}$ have been produced, that appeared to be without defects in studies with XTEM. Second, in contrast to the doping using Er_2O_3 there was no evidence of any lattice strain observed by HRXRD mapping from these ErF_3 doped layers with $N_{\text{Er}} \approx 3 \times 10^{19} \text{ cm}^{-3}$. This result, together with observations of no mosaic broadening, indicates that there was very little lattice distortion introduced by ErF_3 doping.

Er-related luminescence emission around $1.54 \mu\text{m}$ was observed by both PL and EL measurements on these Er/O and Er/F doped Si layers, as shown in Figs. 3 and 4. In general, the Er-related PL emission was intense, as judged by comparing with the observed intensity of the Si-related emissions from the same sample [Fig. 3(a)], at low temperatures. The PL intensity was drastically decreased at measurement temperatures above 150 K. Although this sample was grown

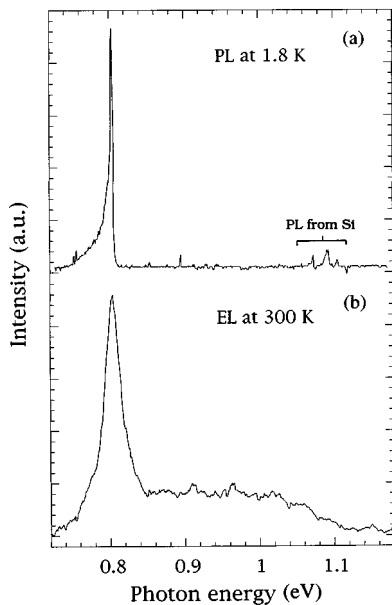


FIG. 3. (a) A wide range PL spectrum from an Er_2O_3 doped sample grown at 420°C , where Er-related PL emission at $1.54\ \mu\text{m}$ is intense compared to the emissions from the Si substrate. (b) An EL spectrum observed at room temperature from the same sample using electron impact excitation.

at 420°C , the temperature limit for the strong thermal quenching is still higher than that from early results of Er doped MBE Si layers that had been annealed at 850°C for 30 min.¹³

The detailed PL line shape of Er/F doped samples is different from that observed from Er/O doped samples, as depicted in Fig. 4. The four different contributions that can be identified in the main peak of the Er/F spectrum are characteristic of a number of single and multiple layer samples doped by the fluoride to concentrations varying by one order of magnitude. In contrast, these fine features are not resolved for oxide doped films. Besides a broader main peak [full width half maximum (FWHM) $\approx 4.5\ \text{meV}$], there is only a broad intensity tail extending towards the low energy side. The relatively broader PL emissions from the Er/O doped structures may be explained as a consequence of the stronger lattice distortion as observed by XRD. These PL results, together with the observed difference in lattice strain between

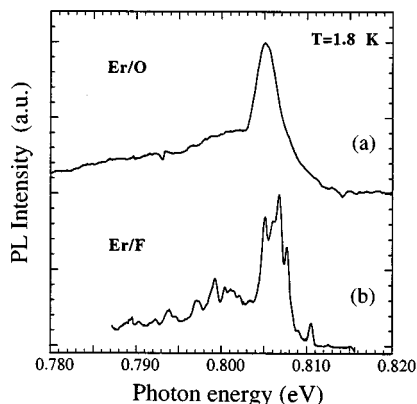


FIG. 4. Comparison of low temperature PL spectra from samples doped with (a) Er/O and (b) Er/F, respectively.

the two types of Er doped samples, imply that there are significantly different complex structures and atomic ligands around the Er atoms in samples doped with Er_2O_3 and ErF_3 , respectively.

EL measurements were performed on some samples doped with Er_2O_3 to $\geq 2 \times 10^{19}\ \text{cm}^{-3}$ using two parallel, $150\ \mu\text{m}$ spaced Al electrodes ($200 \times 500\ \mu\text{m}^2$) on the top surface forming Schottky diodes. When one of these Schottky diodes was strongly reverse biased, Er ions can be excited by injecting hot electrons through an impact process. As shown in Fig. 3(b), rather intense EL at $1.54\ \mu\text{m}$, emitted only from the very small fraction ($\leq 0.1\%$) of the total depletion region around one Al contact, has been observed with a moderate input electric power ($\sim 0.5\ \text{W mm}^{-2}$) at room temperature, indicating that the light emission efficiency from these Er/O doped layers seems high. It is difficult to give an exact value of the quantum efficiency, since the major part of the emission area is covered by the Al layer. Electron impact excitation of Er ions from a Schottky diode was previously only reported by Isshiki *et al.*¹⁴ using Er doped InP materials. The linewidth of the present EL spectrum is broader (FWHM $\approx 27\ \text{meV}$) than that shown in Ref. 16 ($\approx 2.6\ \text{meV}$), but close to those observed from the reverse biased Er doped Si *n-p* junction structures ($\sim 24\ \text{meV}$).^{4,6} At the same time, a characteristic broad background (at $1.10\text{--}0.73\ \text{eV}$, and typically about 20% of the intensity of the $1.54\ \mu\text{m}$ peak at room temperature) is observed in our EL spectra, similar to the EL spectra shown in Refs. 4 and 6, which has been attributed to a so-called bremsstrahlung effect due to hot carrier transitions.⁶

In summary, Er doped Si samples have been prepared using Si-MBE by co-evaporation of Si and Er_2O_3 or ErF_3 . By using a low temperature growth process and optimizing the growth conditions, we have been able to incorporate Er/O and Er/F up to a concentration of $5 \times 10^{19}\ \text{cm}^{-3}$ without Er-related precipitates. Promising luminescence results have been obtained from these Er_2O_3 and ErF_3 doped Si samples.

- ¹ H. Ennen, J. Schneider, G. Pomrenke, and A. Axmann, *Appl. Phys. Lett.* **43**, 943 (1983).
- ² G. Franzo, F. Priolo, S. Coffa, A. Polman, and A. Carnera, *Appl. Phys. Lett.* **64**, 2235 (1994).
- ³ B. Zheng, J. Michel, F. Y. G. Ren, L. C. Kimerling, D. C. Jacobson, and J. M. Poate, *Appl. Phys. Lett.* **64**, 2842 (1994).
- ⁴ J. Stimmer, A. Reittinger, J. F. Nützel, G. Abstreiter, H. Holzbrecher, and Ch. Buchal, *Appl. Phys. Lett.* **68**, 3290 (1996).
- ⁵ Y.-H. Xie, E. A. Fitzgerald, and Y. J. Mii, *J. Appl. Phys.* **70**, 3223 (1990).
- ⁶ S. Coffa, F. Priolo, G. Franzo, A. Polman, S. Libertino, M. Saggio, and A. Carnera, *Nucl. Instrum. Methods Phys. Res. B* **106**, 386 (1995).
- ⁷ A. Polman, J. S. Custer, E. Snoeks, and G. N. van den Hoven, *Appl. Phys. Lett.* **62**, 507 (1993).
- ⁸ R. Serna, J. H. Shin, M. Lohmeier, E. Vlieg, A. Polman, and P. F. A. Alkemade, *J. Appl. Phys.* **79**, 2658 (1996).
- ⁹ M. Matsuoka and S.-I. Tohno, *Appl. Phys. Lett.* **66**, 1682 (1995).
- ¹⁰ W.-X. Ni, J. Ekberg, K. B. Joelsson, H. Radamson, A. Henry, G.-D. Shen, and G. V. Hansson, *J. Cryst. Growth* **157**, 285 (1995).
- ¹¹ K. B. Joelsson, L. Hultman, W.-X. Ni, and G. V. Hansson (unpublished).
- ¹² G. V. Hansson, H. Radamson, and W.-X. Ni, *J. Mater. Sci.* **6**, 292 (1995).
- ¹³ H. Efeoglu, J. H. Evans, T. E. Jackman, B. Hamilton, D. C. Houghton, J. M. Langer, A. R. Peaker, D. Perovic, I. Poole, N. Ravel, P. Hemment, and C. W. Chan, *Semicond. Sci. Technol.* **8**, 236 (1993).
- ¹⁴ H. Isshiki, H. Kobayashi, S. Yugo, T. Kimura, and T. Ikoma, *Appl. Phys. Lett.* **58**, 484 (1991).